ACS FOOD SCIENCE & TECHNOLOGY

Editors' Choice
Open Access

pubs.acs.org/acsfoodscitech

Article

Automatic Chemical Profiling of Wine by Proton Nuclear Magnetic Resonance Spectroscopy

Brian L. Lee, Manoj Rout, Ying Dong, Matthias Lipfert, Mark Berjanskii, Fatemeh Shahin, Dipanjan Bhattacharyya, Alyaa Selim, Rupasri Mandal, and David S. Wishart*

Cite This: ACS Food Sci. Technol. 2024, 4, 1937−1949

Read Online

ACCESS | Metrics & More | Article Recommendations | Supporting Information

ABSTRACT: We report the development of MagMet-W (magnetic resonance for metabolomics of wine), a software program that can automatically determine the chemical composition of wine via ^{1}H nuclear magnetic resonance (NMR) spectroscopy. MagMet-W is an extension of MagMet developed for the automated metabolomic analysis of human serum by ^{1}H NMR. We identified 70 compounds suitable for inclusion into MagMet-W. We then obtained 1D ^{1}H NMR reference spectra of the pure compounds at 700 MHz and incorporated these spectra into the MagMet-W compound library. The processing of the wine NMR spectra and profiling of the 70 wine compounds were then optimized based on manual ^{1}H NMR analysis. MagMet-W can automatically identify 70 wine compounds in most wine samples and can quantify them to 10−15% of the manually determined concentrations, and it can analyze multiple spectra simultaneously, at 10 min per spectrum. The MagMet-W Web server is available at https://www.magmet.ca.

KEYWORDS: *NMR, metabolomics, wine, mixture quantification, automation*

INTRODUCTION

Wine is one of the oldest beverages in the world, with evidence of its production first appearing in a village known as Shulaveris Gora in the Eastern European country of Georgia nearly 8000 years ago.[1] Since its first appearance in the neolithic period, wine has become increasingly integral to many regional diets as well as religious, ceremonial, and cultural activities around the world.[2] Wine is also believed to have a number of health benefits when consumed in moderation (at most 1−2 glasses per day[3]) with protective associations being noted for cardiovascular disease, atherosclerosis, hypertension, certain types of cancer, type 2 diabetes, neurological disorders, and metabolic syndrome.[2,4] Given its long history, its widespread cultural or social importance, and its potential health benefits, wine is now produced, sold, and consumed in >180 countries, with more than 25 billion liters produced per year.[5] This corresponds to a global annual market value of approximately USD $500 billion.[6] Because of wine's high market value, it is important to have a detailed picture of the chemicals contributing not only to its potential health benefits but also to each wine's unique flavor profiles, origins, and details about specific wine faults, additives, or contaminants in wines. Such measures will not only aid in understanding which compounds contribute to a given wine's presumptive health benefits but also help improve wine consistency, enhance quality assurance, offer better traceability, provide improved fraud prevention, and support greater consumer safety.

The chemical characterization of wine has been of interest to not only vintners and oenologists but also to analytical chemists for many decades.[2,7,8] Hundreds of chemicals, including both volatiles and nonvolatiles, are known to be in wines (www.foodb.ca). These contribute to the flavor, appearance, aroma, mouthfeel, sedative/stimulant properties, or nutrient profile of a given wine.[9−12] For instance, ethanol, the second most abundant compound in wine (after water), is responsible for not only the well-known stimulant/sedative effects of alcohol consumption but also the mouthfeel, bitterness, and mild burning sensation experienced when drinking wine. The amount of sugar (e.g., fructose, glucose, and sucrose) in wine is responsible for its dryness (low sugar) or sweetness (high sugar). Wine flavors can also be moderated by the abundance of certain amino acids (e.g., proline and glutamate) which contribute to sweetness or food-like and umami flavors. The tartness and acidity of wine are controlled by its pH and the levels of organic acids (e.g., succinic, malate, lactate, and galacturonate). Other alcohols in wine, such as glycerol, contribute to the viscosity and body of wine, while 2,3-butanediol gives wine a creamy, buttery flavor and 2-phenylethanol gives wine a rose or floral flavor. Certain esters such as ethyl acetate give wine a cherry-like flavor, while ethyl lactate gives wine a fruity flavor. Not all compounds found in wine are beneficial or pleasant. Some can be toxic, such as methanol, while others such as acetate, can give wine a cheesy/sour taste (and may also indicate bacterial contamination), or still others such as such as dimethylsulfone or dimethylamine can be unpleasant and foul smelling.[13−17] Some compounds such as hydroxymethylfurfural have been used to indicate wine storage time.[18] Given their importance in wine quality and

Received: April 18, 2024
Revised: July 2, 2024
Accepted: July 3, 2024
Published: July 22, 2024

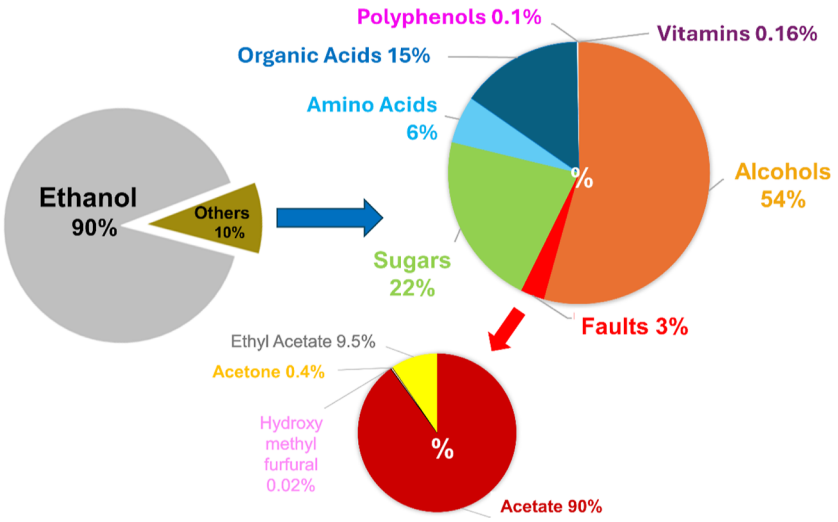

Figure 1. Major metabolites detected in the 1D ^{1}H NMR spectra of four wines (by percentage) automatically identified and quantified by MagMet-W.

taste, the reliable measurement of these compounds gives winemakers another tool to detect batch-to-batch variations in taste, aroma, quality, or contaminant profiles and offer a more consistent, fault-free product. Uncontrolled or undetected batch-to-batch variations can have dire consequences for sales, product valuation, consumer satisfaction, and human health.

To supplement current methods of assessing wine quality, safety, and authenticity, as well as to determine wine varieties or wine provenance, comprehensive, low-cost, high-throughput methods to identify and quantify dozens to hundreds of wine chemicals would be invaluable. A range of techniques can be used to comprehensively characterize the chemical content of wine, including liquid-chromatography mass spectrometry (LC−MS), gas chromatography (GC) MS (GC−MS), inductively coupled plasma (ICP)−MS, capillary electrophoresis (CE), high performance (HP) LC, atomic absorption spectrometry (AAS), Fourier-transform infrared spectroscopy (FT-IR), and NMR. Because of their high sensitivity and widespread compound coverage, the most chemically comprehensive wine analyses are typically MS-based.[13,19−25] However, these MS approaches tend to be expensive and time-consuming (in terms of sample preparation), not intrinsically quantitative, and inherently destructive. More recently, NMR has become a popular approach for characterizing wine.[25−30] Despite being less sensitive and requiring larger sample volumes than MS, NMR has several major advantages: it is cheaper (on a per sample basis), it is far more automated and automatable, it is intrinsically quantitative, it uses simpler sample preparation protocols, and it is nondestructive. While the cost of initially acquiring a high-resolution NMR instrument is much higher than acquiring an LC−MS or GC−MS system, this cost is generally offset by the far lower instrument maintenance costs, the much longer operational lifetime, the lower staffing costs, the higher sample throughput, the ease of complete automation, the cheaper and faster sample preparation, and the lower reagent costs associated with absolute quantification by NMR.

Both targeted and untargeted 1D and 2D ^{1}H- and ^{13}C NMR spectroscopy have been employed for wine profiling.[25−27,29] Wine analysis has also been performed using solid state NMR[31] and benchtop NMR.[32] To date, most in-house approaches to wine analysis by NMR have been very manually intensive with highly variable protocols and relatively inconsistent outcomes.[28] Indeed, manual spectral analyses by NMR can be very time-consuming (30−60 min per spectrum) and can introduce operator's bias and inconsistency in results.[33,34] In an effort to reduce time and improve consistency for NMR-based wine profiling, Bruker Biospin introduced its commercial WineScreener system in 2015.[35,36] The WineScreener system used a modified 400 MHz NMR instrument that is specially adapted for push-button operation. The WineScreener instrument uses a proprietary collection of reference ^{1}H NMR spectra (of both wines and individual wine compounds) and proprietary software to enable the full automation of wine analysis. More recently, Bruker has adapted the WineScreener system to analyze juice, honey, and olive oil so WineScreener is now sold as the FoodScreener. While the Bruker system is highly automated, robust, and intrinsically appealing, it also has its drawbacks. In particular, the system methodology is closed source and confidential, limited in its chemical coverage (due to the low NMR field strength) and not transferable to other NMR instruments or NMR field strengths.

In an effort to overcome these limitations, we developed a fully automated wine analysis software package that is transferrable to almost any existing NMR instrument at almost any NMR field strength. Our approach involves modifying a software package we previously developed called MagMet (http://magmet.ca).[37,38] MagMet is a web-based server capable of completely automated detection and accurate quantification of metabolites from 1D ^{1}H NMR spectra of complex chemical mixtures. We have demonstrated the application of MagMet to the automated analysis of human serum, plasma,[38] and fecal samples.[37] MagMet's data processing is robust and very efficient. It performs automatic Fourier transformation, phase correction, baseline optimization, chemical shift referencing, water signal removal, and peak picking. The program then uses the peak position information from its own standard reference library of ^{1}H NMR spectra to identify and quantify the metabolites via peak pattern matching and spectral deconvolution.[38]

Here, we report further optimization of MagMet to extend its support to wine testing and chemical profiling (called MagMet-W). We have created a comprehensive 1D ^{1}H NMR

https://doi.org/10.1021/acsfoodscitech.4c00298
ACS Food Sci. Technol. 2024, 4, 1937−1949

spectral library (at 700 MHz) of chemicals that can be detected by NMR in wine samples including alcohols, sugars, amino acids, organic acids, esters, and adulterates (Figure 1). Additionally, we have performed complete profiling of 70 wine compounds on four different training wine samples (Sauvignon Blanc, Cabernet Sauvignon, Shiraz, and Concord). We then compared the MagMet-W automated results to manually measured results performed using spectral profiling software (Chenomx[39]). After optimization of the processing and fitting protocols, we found an excellent correlation between the manually identified/quantified compounds and the automatically identified compounds with an overall mean absolute percentage error (MAPE) of 14% and median absolute percentage error of 9%. The processing time is 10 min per spectrum. MagMet-W is available at www.magmet.ca.

MATERIALS AND METHODS

Materials. HPLC grade water, potassium phosphate monobasic (≥99%), potassium phosphate dibasic (≥98%), deuterium dioxide (D_2O, 99.9%), deuterated 2,2-dimethyl-2-silapentane-5 sulfonate (DSS-d_6), potassium disulfite, and Amicon (0.5 mL) 3 kDa molecular weight cutoff (MWCO) filtration units (Millipore, Burlington MA, USA) were purchased from Sigma (Oakville, Canada). 2-Chloropyrimidine-5-carboxylic acid (CPCA, 98%), which is used as a spectral phasing standard, was purchased from ArkPharm (Libertyville, USA). The vendors of the stock compounds used to create the MagMet-W spectral library are listed in Supporting Information Table S1. NMR tubes (3 mm) were purchased from Bruker Ltd. (Milton, Canada). The Chenomx NMR Suite (Version 8.0) NMR metabolomics software, which was used for manual profiling, was purchased from Chenomx Inc. (Edmonton, Canada).

Wine Sample Preparation. Four wine samples were used to develop, refine, and test the MagMet-W algorithm: Oyster Bay Sauvignon Blanc, Barefoot Cabernet Sauvignon, Yellow Tail Shiraz and Manischewitz Concord (see Supporting Information, Table S2). These wines were selected because they were made from different grape varieties, covered a range of wine types (red, white, dessert), and came from different growing regions around the world. Barefoot Cabernet Sauvignon is a red wine made from Cabernet Sauvignon grapes grown in California's Napa Valley. Oyster Bay Sauvignon Blanc is a white wine made from Sauvignon Blanc grapes grown in the Marlborough region of New Zealand. Yellow Tail Shiraz is a red wine made from Shiraz grapes grown in New South Wales, Australia. Manischewitz Concord is a sweet kosher red wine made from Concord grapes grown in the northeastern US. Each wine was purchased locally in Edmonton, Alberta, Canada and stored at room temperature until opened. To further validate the MagMet-W profiling, an additional set of six different wine samples were purchased, each representing a variety of wine types or wine-growing regions and analyzed using the MagMet-W software (see Supporting Information Table S3). Each wine sample was prepared for NMR analysis following the standard procedures for MagMet.[37,38] However, for wine samples, some steps may be best performed with some minor methodological alterations (detailed in the Results and Discussion section). Initially, 0.5 mL of each sample was filtered through a thoroughly prewashed Amicon 3 kDa MWCO centrifugal filter. Next, 200 μL of the filtrate was mixed with 50 μL of 5× NMR buffer (750 mM phosphate buffer pH 7, 5.0 mM DSS-d_6, 5 mM CPCA, and 50% v/v D_2O). The samples were then centrifuged briefly for 5 min and finally 200−250 μL of each sample were loaded into 3 mm SampleJet NMR tubes.

Preparation of Metabolite Standard Solutions. To create the MagMet-W spectral library, stocks of reference compound solutions were prepared for each compound. In particular, 20−40 mM stock solutions of each pure compound were prepared by dissolving it in HPLC grade water (see Table S1). Standard concentrations were determined by weight (as measured on a Sartorius CPA225D microelectronic balance with a precision of 0.0001 g). NMR standard samples were prepared by diluting stock solutions to 1−10 mM. Additionally, to generate the reference sample of acetaldehyde bisulfite, a 5-fold excess of potassium disulfite was added to an acetaldehyde solution. To prepare the reference compounds for NMR acquisition, 200 μL of each sample was transferred to a 1.5 mL microcentrifuge tube and mixed with 50 μL of 5× NMR buffer. Consequently, each NMR sample contained 150 mM phosphate buffer, 1.0 mM DSS-d_6, 1.0 mM CPCA, and 10% D_2O. The pure compound stock solutions were also used to spike samples of white and red wine to assist in the identification of peaks in the NMR spectra. For these spiking experiments, samples of wine in an NMR buffer were prepared as described above, with the additional step of spiking each wine sample with an appropriate amount of pure compound solution. The compound spiking was performed after the filtration step but before the addition of the NMR buffer. Comparison of the peak intensities in the NMR spectra of wine samples with and without compound spiking helped to identify the correct peak positions for the spiked compound.

NMR Spectroscopy. All 1D ^{1}H NMR spectra for the library reference compounds and wine samples were acquired using a Bruker AVANCE III 700 MHz spectrometer (Bruker Biospin, Rheinstetten, Germany) equipped with a triple resonance 5 mm CryoProbe. Samples in NMR tubes were centrifuged for 1 min at 800 × g to remove bubbles and were stored in an NMR autosampler (SampleJet Bruker) set at 4−10 °C. Each sample was prewarmed to 25 °C before insertion into the spectrometer. All samples were locked using the D_2O signal, and the probe was matched and tuned. Each sample was shimmed individually by using the automated routines available in the TopSpin software (version 3.6.2). Shimming was performed to achieve a symmetric DSS peak with a peak width of less than 1 Hz. All 1D ^{1}H NMR spectra were obtained using a 1D ^{1}H-NOESY (noesypr1d) pulse sequence, with a 2 s recovery delay with low-power presaturation for water suppression, a 50 ms mixing time with water saturation, and a 4 s acquisition time. The transmitter frequency was set to 4.7 ppm, and the sweep width was set to 12 ppm. The gain and pulse widths were calibrated automatically for each sample by the software. Eight dummy scans were used, after which 128 transients were collected. The same parameters were used for all of the spectra. Spectra were reacquired or the samples remade in case of poor line shape quality or line width higher than 1 Hz.

For the comparative performance studies, NMR spectra acquired for wine sample analysis (using the protocols described above) were manually processed and profiled using the Chenomx NMR Suite (Version 8, Chenomx, Inc., Alberta, Canada). Specifically, the 1D ^{1}H-NOESY spectra were processed using the Chenomx software. The spectra were zero-filled to at least twice the original data size, and exponential line broadening was applied such that the DSS peak width was 1 Hz. In all cases, a manual baseline correction was applied. For manual profiling, wine samples were quantified using a combination of the Chenomx-provided 700 MHz compound library and an in-house compound library acquired at 700 MHz. Concentrations reported in this article (μmol/L) have been corrected for dilution with the NMR buffer.

Developing the NMR Wine Spectral Library and the MagMet-W Software. Individual 1D ^{1}H NMR reference spectra for each of the 70 identified wine compounds were obtained using the NMR spectral collection parameters described above and as described elsewhere.[37,38] The concentrations of each metabolite were determined via precision weighing. The spectra were processed using TopSpin (version 4.0.6) and converted into XML formatted files (using a specially developed in-house program called NMRLib) to capture information about peak positions, cluster positions, peak intensities, and peak widths for each compound. All reference NMR spectra used in the MagMet-W spectral library had to meet certain minimal standards (Lorentzian line shapes, line widths <1 Hz, flat baseline, proper phasing, etc.), and if they failed, the spectra were reacquired.

The algorithm, design and testing of the MagMet software was described previously.[37,38] MagMet is a 1D ^{1}H NMR spectral processing and spectral deconvolution program written in Python

https://doi.org/10.1021/acsfoodscitech.4c00298
ACS Food Sci. Technol. 2024, 4, 1937−1949

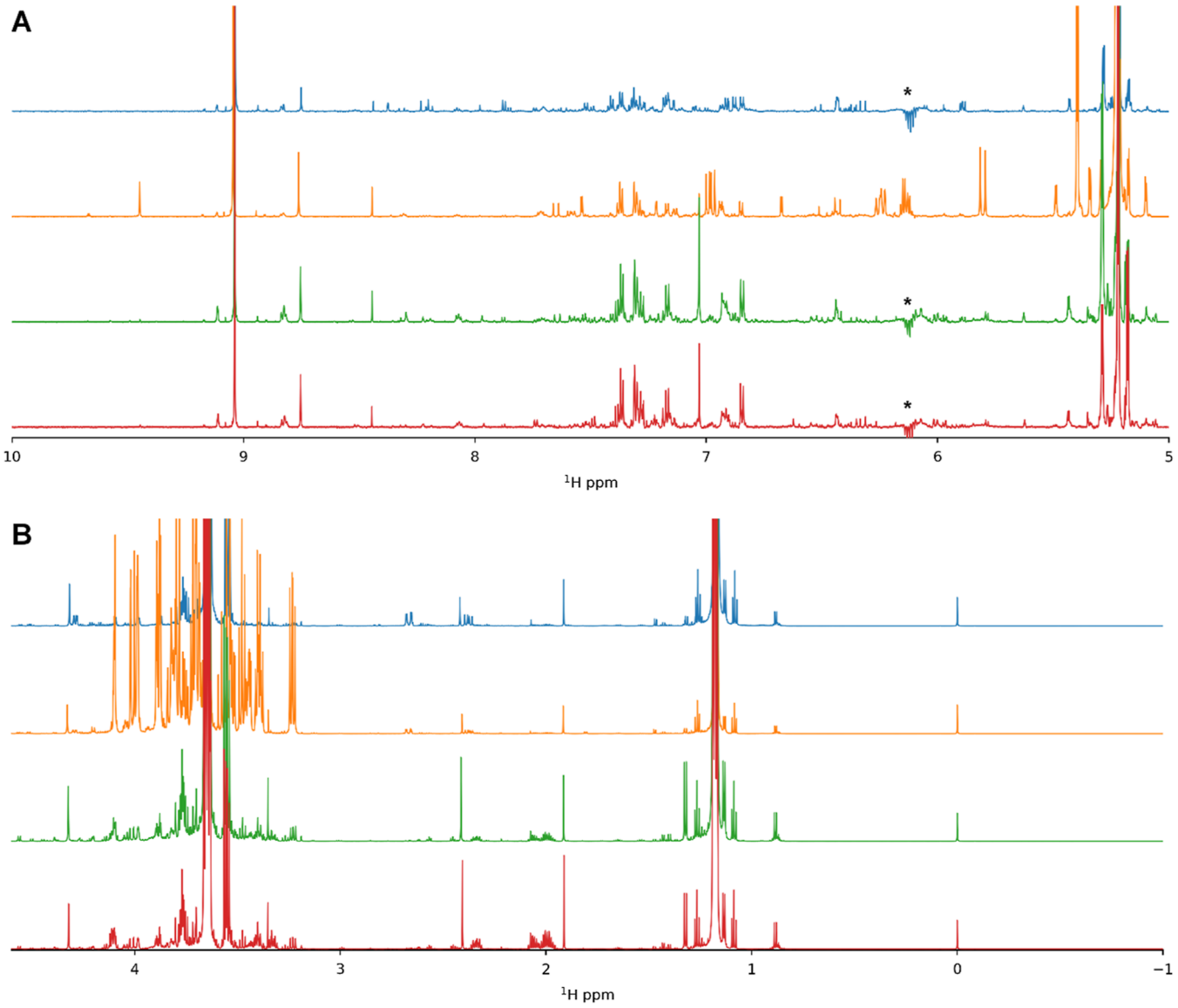

Figure 2. 1D ^{1}H NMR spectra of wine samples. Wine samples were prepared as described in Materials and Methods, with ultrafiltration, a strong phosphate buffer at pH 7, and DSS and CPCA (singlets at 0.00, 9.04, and 8.75 ppm) used for referencing and automated processing of the spectra. The aromatic region (A) is shown at a 100× higher scale compared to the aliphatic region (B). The samples represent from top to bottom: Sauvignon Blanc (blue), Concord (orange), Shiraz (green), and Cabernet Sauvignon (red). The asterisk denotes a spectral artifact we observe in our spectra.

(version 3.11) that makes use of functions contained in the NMRGlue[40] package (version 0.9) to facilitate spectral processing. Additional Python functions have been written to support automated phasing, baseline correction, water removal, chemical shift referencing, and peak picking. Spectral deconvolution is performed through comparisons and iterative fitting between the spectral peak list and the compound peak lists in the MagMet-W spectral library. A web-based interface to the MagMet-W profiling software was developed using the Ruby on Rails web framework, which manages the submission and queueing of the automatic processing and profiling. The Web site also includes an in-house developed NMR spectrum viewer (called JSpectraViewer[41]) which can be used to visualize and manually adjust the results of the automated profiling by MagMet-W. After construction and optimization of MagMet-W was completed, the new version of the software was ported to the MagMet Web server, located at https://www.magmet.ca.

RESULTS AND DISCUSSION

Wine Sample Preparation. Several different protocols for preparing wine samples for NMR analysis have been described or proposed including liquid−liquid extraction, solid-phase extraction or drying/lyophilization (to remove ethanol).[11,26,27] To ensure compatibility with our existing spectral library of compounds for analyzing serum and fecal water, we followed similar procedures for NMR sample preparation that we used previously for MagMet.[37,38] The first step in our standard sample preparation process involves ultrafiltration of the samples. This helps remove particulates such as tartaric acid crystals or other precipitates as well as higher molecular weight compounds such as proteins or lipids, which can affect the overall quality of the NMR spectrum. While the samples used in this study were filtered, we have since found that the filtration step has minimal effect on the NMR spectra of wine (Figure S1), and so the filtration step can likely be omitted for

https://doi.org/10.1021/acsfoodscitech.4c00298
ACS Food Sci. Technol. 2024, 4, 1937−1949

most wine samples. Some NMR protocols lyophilize wine samples to remove ethanol,[42−44] which dominates the spectrum and prevents analysis of spectral peaks near the ethanol peaks. Our sample preparation protocol did not use lyophilization, since it can also remove important volatile compounds.[45] When a strong phosphate buffer was added to our samples, the pH of the wine samples ranged between pH 6 and 7, as measured by a pH meter. This pH shift was also independently confirmable by the chemical shift of the acetate peak which, for these samples, ranges from ∼1.91 to 1.92 ppm as expected for acetate in its basic form.[46] The pH of wines normally varies between 2 and 4 and is dependent on numerous factors including grape quality, fermentation conditions, and the quantity of acidic compounds present. The use of a strong phosphate buffer helps to normalize the pH of the samples, thereby reducing variation in the NMR spectra from the movement of peaks that originate from pH-sensitive compounds.

As shown in Figure S2, there are large chemical shift changes (up to 0.4 ppm) between the NMR spectra of wines at pH 7 and those of wines at pH 3, which can be attributed to pH-sensitive compounds (due to protonation). Other compounds (sugars, alcohols) show little or no chemical shift change. While the wine spectra cannot be perfectly superimposed after the buffering step, the chemical shifts typically differ from their reference values by a very small amount (<0.02 ppm) which is sufficient for reliable identification of these compounds using both Chenomx and MagMet-W. The neutral pH also allows us to better match the standard Chenomx compound library and our own custom library of standard compounds, which were developed for human biofluids at a pH of 7.0−7.4.

For the compounds measured in this paper, the solubility and stability do not appear to be different at pH 7 versus pH 3. However, some compounds, such as glucose and acetaldehyde, exist in a pH induced equilibrium between different forms in solution. The interconversion between these forms and the ratio between these forms is significantly influenced by pH. Therefore, a consistent pH between the reference standards and the wine samples is necessary for accurate quantification. For other compounds, such as malate, the change in protonation state with pH can influence this compound's ability to coordinate metal ions. This can lead to differences in chemical shifts or line widths at different pH values, or depending on the sample contents, between different samples. Again, choosing a consistent sample preparation methodology can help minimize these differences. MagMet-W's quantification algorithm assumes that compounds such as malate are not coordinated. As discussed later, the MagMet-W interface offers the ability to visually inspect the results and identify any issues that may influence compound quantification. The buffer also includes 1.0 mM DSS as an internal concentration and chemical shift standard, as well as CPCA with a well-resolved peak at 9.04 ppm, which is used as a phasing standard by MagMet.

As noted earlier, all wine samples were centrifuged to bring down any residual liquid on the sides of the sample containers as well as to ensure that the samples were free of precipitates (if any) before loading the samples into NMR tubes. We did observe some precipitate, which we speculate could be due to the formation of magnesium and calcium phosphates (which do not affect the ^{1}H NMR spectra). The potassium present in our buffers may also cause the precipitation of tartarate, as discussed later. Finally, we used 3 mm NMR tubes which require smaller volumes (∼200−250 μL) and provide increased sensitivity for samples of high iconic strength (common for biological samples), particularly for cryprobes.[47] However, the procedures outlined above and the MagMet software are fully compatible with more common 5 mm tubes, although 600−700 μL of total sample would be required.

The 1D ^{1}H-NOESY pulse sequence was chosen for its simplicity and for its good water suppression properties.[48] It was also chosen for consistency with our established library of compounds (which were also obtained by using the same 1D ^{1}H-NOESY experiment). Since the samples were run using our NMR instrument's full automation mode, every sample had automated gradient shimming to ensure that the spectral quality was sufficient for automated peak picking and fitting by MagMet-W. It also ensured that the sample spectral quality matched the spectral quality used for the reference library. The 1D ^{1}H NMR spectra of the four wines used for training and refining the MagMet-W algorithm are shown in Figure 2. As expected, the ethanol signal was dominant in all spectra (at 1.18 and 3.65 ppm). The ethanol peak also created an artifact at 6.10−6.15 ppm that appeared as a negatively phased multiplet. This artifact appears to be correlated with the level of the ethanol concentration in the NMR samples; lower ethanol concentrations (such as in beer), do not exhibit this spectral artifact. We speculate that this spectral aberration may be a quadrature artifact, as it appears in a position opposite to the ethanol CH_2 signal. The internal CPCA standard gave a well resolved singlet at 9.04 ppm and a second singlet from an impurity at 8.75 ppm and the internal DSS standard yielded a well-resolved singlet at 0.00 ppm.

Calibration, Referencing and Optimization for MagMet-W. To create a MagMet-compatible spectral library for wine analysis, three steps were taken. First, NMR detectable chemicals in wine were identified through a review of the literature[11,28,30,36,45,49−61] and from prior NMR wine studies in our lab. These previous studies identified wine chemicals through manual profiling using Chenomx software and its standard chemical library. Second, the Chenomx NMR Suite 8.0 library was manually expanded by collecting NMR reference spectra for wine compounds not already in the Chenomx standard library. This was done following protocols described in the Chenomx software manual. The concentrations of the compounds in the reference spectra were determined from the weight (if a solid) or volume (if a liquid) of the compound that was used to prepare each of the stock solutions. The ratio between the intensities of the compound peaks and an internal standard were used to determine the concentration in the wine samples with the same peaks, so long as the spectra were acquired with the same pulse sequence parameters.[39] This procedure for quantification, which is used for both Chenomx and MagMet-W, contrasts with "qNMR" methods, where concentrations are determined directly by the integration of the signals. However, qNMR requires that spectra be acquired using long delays (30−60 s) and consequently long acquisition times (1−2 h). Third, the wine spectra for the four training wines were manually profiled by using the expanded Chenomx library to determine which compounds could be reliably identified and quantified. Spiking experiments were performed for compounds that were difficult to identify from the wine samples alone. These experiments helped to reveal the correct position of the compound peaks, allowing for their accurate identification. Several examples are shown in Figure S3. Notably we found additional unexpected

https://doi.org/10.1021/acsfoodscitech.4c00298
ACS Food Sci. Technol. 2024, 4, 1937−1949

Table 1. Table of Wine Compounds and Their Concentrations in mg/L Determined by Automatic Spectral Profiling Using MagMet-W[a]

HMDB	name	median	range	literature	ref[b]
HMDB00108	ethanol	74,210	58,182−107610	71,010−102570	62
HMDB00131	glycerol	7074	3456−12007	7000−10000	
HMDB00660	fructose	5226	117−69835	200−4000	
HMDB00122	glucose	2884	94−52103	500−1000	
HMDB00956	tartarate	1044	721−1608	2000−6000	
HMDB00190	lactate	764	73−2055	0−3000	
HMDB00254	succinate	710	216−1017	500−1000	
HMDB03156	2,3-butanediol	619	278−1283	200−3000	65
HMDB02545	galacturonate	509	106−1935	100−1000	
HMDB00162	proline	500	179−2692	0−4000	
HMDB00156	malate	453	36−4003	2000−7000	
HMDB00211	myo-inositol	380	173−817	220−730	66
HMDB00042	acetate	338	200−877	100−500	
HMDB06007	isoamylalcohol	169	79−307	84−333	
HMDB00646	arabinose	148	40−586	500−1000	
HMDB00975	trehalose	116	53−444	5−250	67
HMDB01875	methanol	112	17−258	21−194	
NA	acetaldehyde (bisulfite)	88	6−214	30 ± 70	64
HMDB40735	ethyl lactate	86	4−320	5−50	
HMDB00606	2-hydroxyglutarate	69	14−135		
HMDB00098	xylose	67	14−314	4−41	67
HMDB00143	galactose	48	19−137	0−100	
HMDB33944	phenylethanol	46	14−72	40−153	
HMDB31527	2-methylbutanol	42	14−82	16−31	
HMDB00112	4-aminobutyrate	31	0−56	0−580	
HMDB00161	alanine	30	0−165	0−200	68
HMDB04284	tyrosol	29	11−39	20−60	69
HMDB00820	propanol	28	14−81	11−125	70
HMDB00097	choline	27	5−43	34−45	71
HMDB06006	isobutanol	27	12−65	25−87	
HMDB03070	shikimate	26	0−74	3−36	72
HMDB00267	pyroglutamate	24	9−69	0−610	73
HMDB31217	ethyl acetate	20	1−86	5−63	
HMDB05807	gallate	19	1−52	0−70	
HMDB00208	oxoglutarate	18	10−101	0−74	
HMDB00062	carnitine	17	1−48		
HMDB00094	citrate	16	3−135	100−700	
HMDB13680	caftarate	16	7−51	0−40	
HMDB03243	acetoin	13	2−47	0−60	
HMDB00191	Aspartate	13	0−20	19 ± 16	74
HMDB00149	ethanolamine	13	4−24	4−17	75
HMDB00687	leucine	11	0−39	0−32	68
HMDB00875	trigonelline	11	5−22	5−43	76
HMDB00159	phenylalanine	10	2−22	0−38	68
HMDB00158	tyrosine	8	0−16	0−30	68
HMDB00168	asparagine	7	1−27	0−42	68
HMDB02780	catechin	7	0−24	15−45	
HMDB00243	pyruvate	6	0−28	0−25	
HMDB00296	uridine	6	2−20		
HMDB00043	betaine	6	0−11	10	77
HMDB00696	methionine	5	2−9	0−14	68
HMDB00214	ornithine	5	0−11	0−74	78
HMDB00671	indole-3-lactate	5	1−22		
HMDB02085	syringate	5	0−12	7−590	79
HMDB00300	uracil	4	0−8		
HMDB01871	epicatechin	4	0−26	10−65	
NA	1,3-propanediol	3	0−7		
HMDB00142	formate	3	1−6	20−90	80
HMDB01964	caffeate	3	0−15	0−2	81
HMDB02322	cadaverine	3	0−15	0−3	82

https://doi.org/10.1021/acsfoodscitech.4c00298
ACS Food Sci. Technol. 2024, 4, 1937−1949

Table 1. continued

HMDB	name	median	range	literature	ref[b]
HMDB00034	adenine	2	0−9		
HMDB00060	acetoacetate	2	1−3		
HMDB34355	5-hydroxymethyl-2-furancarboxaldehyde	1	0−29	1−74	
HMDB29581	sorbate	1	0−175	0−200	83
HMDB00134	fumarate	1	0−2	0−600	84
HMDB01659	acetone	1	0−4		
HMDB00056	beta-alanine	1	0−22		
HMDB00258	sucrose	0	0−1410	0−200	
HMDB00954	ferulate	0	0−6	0−2	85
HMDB00990	acetaldehyde (free)	0	0−2	1 ± 1	63

[a]Example ranges from the literature are also provided. [b]From ref 62 unless otherwise stated.

changes to the NMR spectrum after spiking with acetaldehyde, which appeared to be assignable to the bisulfite adduct of acetaldehyde (Figure S3B−D).

In total, 70 compounds were identifiable in the four training wine samples. The compounds, their median concentrations, and ranges, along with their expected values from the literature, are listed in Table 1. The pie chart in Figure 1 summarizes the metabolites and metabolite classes present in these wines. While most of the 70 compounds were common to all four training wines, they were present in different amounts (Table S2). As expected, the ethanol concentration dominated the NMR spectra (Figure 1), with three of the wines having ethanol concentrations in the ∼12−15% range (Table S2), while the Concord wine contained a lower ethanol concentration of ∼7%. Most of the wines are quite dry, with low sugar (glucose plus fructose) concentrations in the 4−10 g/L range (Table S2), while the Manischewitz wine shows a much higher sugar concentration (120 g/L) due to fortification with high-fructose corn syrup. Amino acids, such as proline and glutamate, which contribute to some of the more complex flavors in wine, were detected in all wines. Organic acids such as malate, tartarate, and succinate, responsible for tart or sour taste of wine, were also identified in all four wines (Table 1). We note that the tartarate concentrations in our samples appear to be low (0.7−1.6 mg/L) compared to the typical concentrations reported in wine (2−6 mg/L). Our protocol for buffering wine samples uses a potassium phosphate buffer. However, it is known that tartarate can precipitate in the presence of potassium, which likely results in the lower-than-expected concentrations observed here. The use of a sodium phosphate buffer, instead of a potassium phosphate buffer as used in this study, could reduce the degree of precipitation and may provide more accurate tartarate concentrations. We also identified sorbate, a common preservative, in Concord wine. Several compounds that could potentially be a wine fault including acetate and acetone were found in all four wines. Hydroxymethylfurfural, an indicator of the time wine has spent on the shelf,[18] was also present in varying levels in all four wines. We were also able to confirm the presence of the bisulfite adduct of acetaldehyde in our samples, even when no free acetaldehyde could be observed. Such sulfite adducts result from the addition of potassium metabisulfite or SO_2 gas to wines as a preservative.[62−64] Overall, these 70 compounds accounted for 55% of the area of the aromatic region and 95% of the area of the aliphatic region.

Optimization of MagMet for Wine Profiling. After identifying 70 reliably measurable wine compounds through manual profiling, we then determined if our earlier versions of MagMet[37,38] could correctly process the wine NMR spectra. We found that the original MagMet could indeed process wine spectra but needed slight modifications. MagMet normally uses the peaks originating from the DSS and CPCA to determine the correct phasing parameters for each ^{1}H NMR spectrum. However, small errors in the phasing of DSS and CPCA are amplified in the much larger ethanol peaks found in wine, which resulted in slightly out-of-phase peaks for ethanol. This affected the baseline correction step. To correct this error, an additional phasing step was added to the MagMet-W algorithm to identify the large ethanol peaks and further refine the phasing parameters using those out-of-phase peaks. This ethanol phasing correction resulted in a much better-quality NMR spectrum. The original version of MagMet would then adjust the baseline by iteratively attempting to separate signal and baseline regions and then fit the baseline regions to a smooth curve. We found that we needed to specifically ignore a negatively phased artifact at 6.10 ppm that appears to be caused by the large ethanol signal (Figure 2A). For baseline correction, MagMet-W assumes that all of the peaks are positive, except for the water region (which is excluded during baseline correction). MagMet-W does not handle negative peaks. Therefore, this region was excluded from the baseline correction algorithm.

The next step was to assemble the MagMet-W wine library consisting of ^{1}H NMR spectra for the 70 compounds identified by manual profiling. Spectral library files for compounds that were common to other biofluids in MagMet were reused, while spectral library files for wine-specific compounds were collected. Due to the high concentration of ethanol in wine, the ^{13}C satellite peaks were included in the ethanol spectral library files.

The MagMet-W wine spectral library data and spectral fitting parameters were then optimized to give the best visual fit of the expected peak cluster positions and intensities for the corresponding compounds. In general, the optimization involved careful, manual adjustment of the chemical shift ranges of peak clusters to properly identify the peak cluster positions as well as the weighing of particular regions of the NMR spectrum more than others to properly fit the observed spectral intensities. Despite the normalization of sample pH (to 7.0) and chemical shift referencing to DSS, we observed variations in several peak positions in the wine spectra. Notably, the sugar (glucose and fructose, Figure 3A) and ethanol chemical shifts (Figure 3B) appeared to have a dependence on sugar and/or ethanol concentration. We speculate that these chemical shift changes are due to "matrix effects" on the DSS molecule and various metabolites in the

https://doi.org/10.1021/acsfoodscitech.4c00298
ACS Food Sci. Technol. 2024, 4, 1937−1949

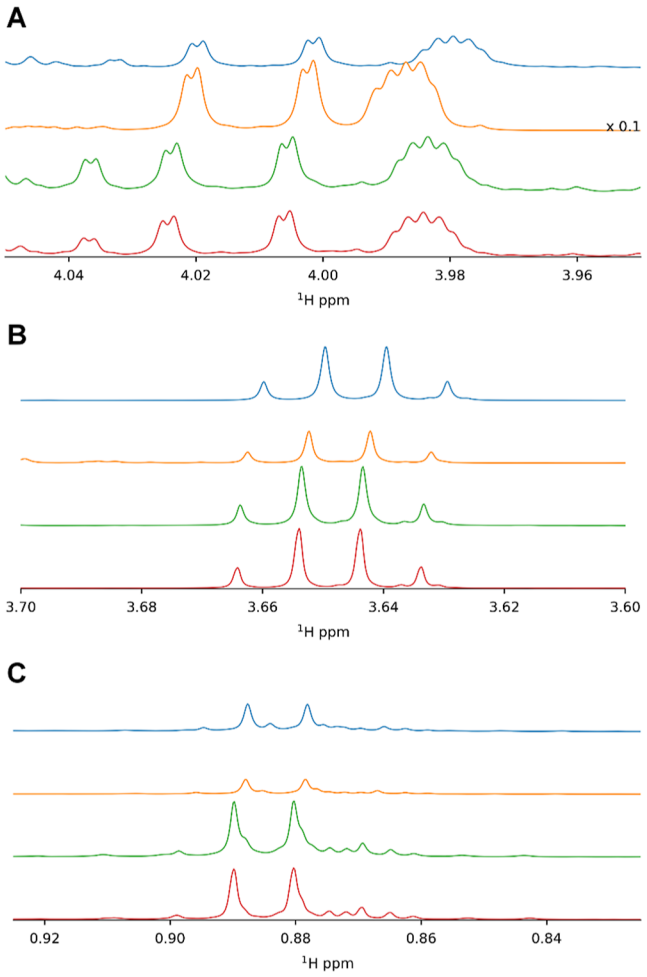

Figure 3. Sample-dependent chemical shifts and line broadening effects in the four wine samples: Sauvignon Blanc (blue), Concord (orange), Shiraz (green), and Cabernet Sauvignon (red). Spectra are normalized and referenced to the DSS peak at 0.00 ppm. (A) Fructose, (B) ethanol, (c) isoamyl alcohol (doublet, ~0.88−0.89 ppm), and other alcohol methyl groups.

sample. We suspect weak interactions between various molecules and ions in different samples can cause subtle sample-to-sample variations in the chemical shifts of the measured molecules. Similar chemical shift changes are also evident in the methyl region of most wines (Figure 3C). However, as these shifts were small, careful adjustment or expansion of the cluster chemical shift ranges in MagMet enabled their proper identification without the need for any additional spectrum or peak alignment.

After optimizing the spectral processing, MagMet-W spectral library files, and fitting parameters for wine, we obtained an excellent fit to the wine spectra for the given reference compounds. An example fit from one of the wines (Sauvignon Blanc) is shown in Figure 4. Figure 4A shows the fit of the aromatic region, including amino acids such as phenylalanine and tyrosine, phenolic compounds such as phenylethanol, caftarate, and ferulate, and the aromatic precursor shikimate. Figure 4B shows the anomeric region with the major reducing sugars (glucose, xylose, trehalose, and galacturonate) identified. Figure 4C highlights the aliphatic region with glucose, fructose, ethanol, and glycerol as well as tartarate and malate. Figure 4D shows proline and a number of organic acids, including malate, succinate, and acetate. Figure 4E shows the methyl region of the NMR spectrum, containing the second ethanol peak and various organic acids, amino acids, and alcohols, with 2,3-butanediol being the most prominent. A number of peaks, notably in the aromatic region, are as yet unidentified. Further work is ongoing in our laboratory to identify these peaks.

As a final step, the optimized wine spectral library along with MagMet-W was added to our publicly available server at www.magmet.ca, and the four wine spectra were uploaded for automatic processing and profiling. The MagMet-W server runs on an 8 × 1.8 GHz CPU and so is currently capable of analyzing up to 8 spectra simultaneously. The analysis of the wine spectra takes an average of 10 min per spectrum on the server. This is significantly faster than the 30−60 min per spectrum generally required for manual processing and quantification. Additionally, MagMet-W can be set up to analyze multiple spectra in parallel, resulting in a further increase in the throughput.

Comparison of Manual Profiling with MagMet-W. To assess the accuracy and correctness of the compounds identified and concentrations obtained by MagMet-W, we compared the MagMet-W results with the Chenomx manually profiled results. A plot of the measured concentrations for the four wine samples is shown in Figure 5. Overall, the correlation is excellent, with an R^2 value of 0.9997, an MAPE of 14% (root-mean-square error or RMSE of 20%) and a median absolute percent error of 9%. Using the Jaccard similarity coefficient, which quantifies the average overlap between the metabolites detected (or not detected), a score of 96% between MagMet-W and Chenomx profiling was obtained (using compounds with levels >10 μmol/L). Using sensitivity and specificity scores, where the compounds identified via manual profiling were considered the gold standard, an average sensitivity of 97% and specificity of 94% were obtained. These results suggest that MagMet-W is somewhat conservative in compound identification, with a bias toward false negatives, but few false positive identifications.

A closer examination of the spectra in Figure 4 and concentrations in Figure 5 shows small discrepancies with the concentrations in the experimental spectrum, the Chenomx manually determined concentrations, and the MagMet-W determined values. The MagMet-W fit (Figure 4) shows that some simulated clusters are slightly misplaced, relative to the true cluster position. This happens because MagMet-W is unable to identify the peaks for a particular cluster because other peaks overlap and obscure the peaks in that compound. For example, around 3.75 ppm, the upfield CH_2 satellite of ethanol and the Hα peak of proline are partly obscured by peaks from glycerol and fructose, respectively. However, their concentrations are still correctly determined because other sufficiently resolved peak clusters, for example, the Hγ and Hδ peaks for proline at 2.0 ppm, can be used by MagMet-W for quantification. Galactose is occasionally underestimated by MagMet-W (Figure 5). Notably for the Concord wine, this appears to be a result of a downfield shift of the anomeric doublet around 5.25 ppm. This results in a misassignment by MagMet-W of one of the two peaks in the doublet to a smaller peak in the same region. For pyroglutamate, beta-alanine, and asparagine, the differences appear to result from differences in baseline correction between the two programs, with MagMet-W having a preference for a slightly stronger baseline correction. Differences in baseline correction between MagMet-W and Chenomx and inconsistencies in baseline

https://doi.org/10.1021/acsfoodscitech.4c00298
ACS Food Sci. Technol. 2024, 4, 1937−1949

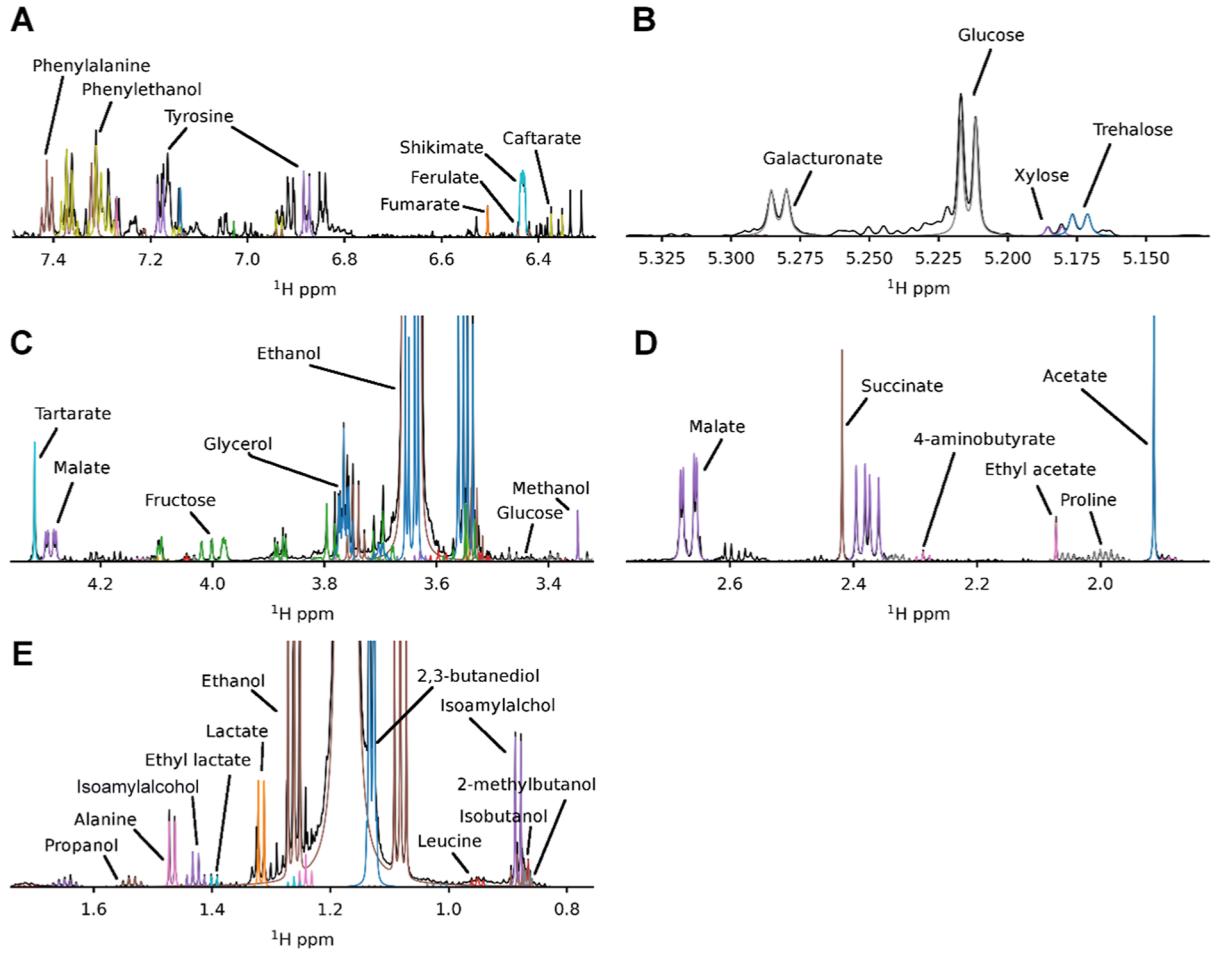

Figure 4. Example fit of a ^{1}H NMR spectrum of a Sauvignon Blanc sample by MagMet-W's automatic profiling algorithm. The observed spectrum is shown in black, while the individual peak clusters identified by MagMet-W are shown in color and labeled. (A) Aromatic region. (B) Anomeric region. (C,D) Aliphatic region. (E) Methyl region.

correction and profiling in Chenomx are likely the main source of error in NMR-based quantification. We estimate these errors contribute significantly to the median 9% error described above. The errors in cadaverine and pyruvate concentrations appear to be due to peak overlap. Cadaverine overlaps with 4-aminobutyrate at 3.0 ppm. While 4-aminobutyrate can be quantified using a well-resolved peak at 2.29 ppm, cadaverine has no other well-resolved peaks that can reliably constrain the concentration of cadaverine. Pyruvate yields a single peak around 2.36 ppm. However, this peak in the Sauvignon Blanc sample overlaps with the malate signal, forming a shoulder on the low-ppm side of the malate peak. While this shoulder can be easily fit manually using Chenomx, it is more difficult for MagMet-W to automatically detect and fit such a doublet. In other wine samples, the relative positions of malate and pyruvate (perhaps due to concentration or pH differences between the samples) result in well resolved or fully overlapped peaks which were accurately fit by MagMet-W. The MagMet-W Web site has an interactive spectral viewing/editing interface that enables underfit or overfit peaks to be quickly identified and manually adjusted.

To further validate the optimized MagMet-W profiling, we acquired 1D ^{1}H NMR spectra for an additional set of six wine samples. These wine samples were not used in the original software development and optimization process. The measured compound concentrations are shown in Table S3, and a comparison of the manual Chemomx results with the automatic MagMet-W profiling results is shown in Figure S4. Overall, the MAPE for these additional wine samples was 12% (RMSE 18%, median 9%) with a R^2 of 0.9980, similar to that in the training set.

LIMITATIONS

As highlighted in our previous MagMet publications,[37,38] and in this paper, MagMet is not without some limitations in its ability to profile serum, aqueous fecal extracts, and wine spectra. To ensure consistency and reproducibility, specific and consistent methods must be followed to prepare wine samples and to acquire NMR data. While the wines were filtered for this study, more recent work suggests that filtering is unnecessary. All wine samples need to be buffered to pH ~ 7 to match the MagMet-W reference library. Due to possible issues with precipitation of tartarate, we suggest using sodium phosphate rather than potassium phosphate. Finally, wine samples must be well shimmed, and the acquired NMR spectra need to have good line shapes and sufficient signal-to-noise ratios for the proper detection and identification of peaks. While we have made every effort to optimize MagMet-W for automatic analysis of a variety of wine samples, we recommend manually inspecting the spectra for obvious misplaced or poorly quantified peaks. The interactive spectral viewer (called JSpectraView) included in the MagMet web interface enables

https://doi.org/10.1021/acsfoodscitech.4c00298
ACS Food Sci. Technol. 2024, 4, 1937−1949

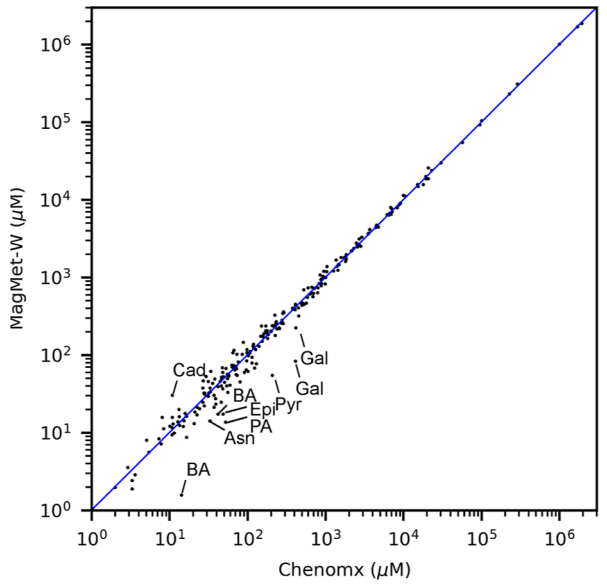

Figure 5. Correlation (R^2 = 0.9997) between concentrations of the 70 compounds measured by Chenomx and MagMet-W in the NMR spectral profiling of the four "training" wine samples. Outliers are labeled. Abbreviations: Asn, asparagine; BA, beta-alanine; Cad, cadaverine; Epi, epicatechin; Gal, galactose; PA, pyruvic acid; Pyr, pyroglutamate.

users to easily and quickly check the automated profiling results. It also allows users to manually adjust the peak positions and the peak intensity of each compound. For spectra submitted through the web interface, these changes are saved. MagMet-W data can also be saved to a local computer and visualized by dragging and dropping the file into the viewer. Adjustments to local files are not saved, however. The current version of MagMet-W only supports the analysis of ^{1}H NMR spectra from 700 MHz NMR spectrometers. Work on expanding and optimizing the MagMet-W for other NMR spectrometer frequencies is in progress.

In conclusion, we have successfully created, tested, and validated a software package called MagMet-W that automatically processes 700 MHz ^{1}H NMR spectra of wine and produces accurate, quantitative read-outs of a large number of wine compounds. In particular, MagMet-W is able to identify and quantify up to 70 compounds that are commonly found in wine, with a quantification accuracy comparable to trained experts. We believe that MagMet-W will be of value in NMR studies and analysis of wine, as its automated nature makes it suitable for high throughput applications for commercial wine testing, wine quality control assessment, and wine evaluation. We estimate that the costs of comprehensive wine analysis via MagMet-W would be as little as USD $10 per sample and that an NMR facility equipped with a standard autosampler could easily process 80−90 wine samples a day. MagMet-W is available at www.magmet.ca.

■ ASSOCIATED CONTENT

Supporting Information

The Supporting Information is available free of charge at https://pubs.acs.org/doi/10.1021/acsfoodscitech.4c00298.

Materials−chemicals and their vendors; tables of metabolites quantified in each of the wines used to optimize and validate MagMet-W; and figures showing NMR spectra from filtered and unfiltered wine, wines at pH 7 and pH 3, as well as spiking experiments and comparing Chenomx manual profile to MagMet-W automated profiling of different wines (PDF)

■ AUTHOR INFORMATION

Corresponding Author

David S. Wishart − *Department of Biological Sciences, University of Alberta, Edmonton T6G 2E9, Canada; The Metabolomics Innovation Centre (TMIC), Edmonton T6G 2E9, Canada; Department of Computing Sciences, University of Alberta, Edmonton T6G 2E8, Canada; Department of Laboratory Medicine and Pathology, University of Alberta, Edmonton T6G 2B7 AB, Canada; Faculty of Pharmacy and Pharmaceutical Sciences, University of Alberta, Edmonton T6G 2H7 AB, Canada;* orcid.org/0000-0002-3207-2434; Phone: 1-780-492 8574; Email: dwishart@ualberta.ca

Authors

Brian L. Lee − *Department of Biological Sciences, University of Alberta, Edmonton T6G 2E9, Canada*

Manoj Rout − *Department of Biological Sciences, University of Alberta, Edmonton T6G 2E9, Canada*

Ying Dong − *Department of Biological Sciences, University of Alberta, Edmonton T6G 2E9, Canada*

Matthias Lipfert − *Department of Biological Sciences, University of Alberta, Edmonton T6G 2E9, Canada*

Mark Berjanskii − *Department of Biological Sciences, University of Alberta, Edmonton T6G 2E9, Canada*

Fatemeh Shahin − *Department of Biological Sciences, University of Alberta, Edmonton T6G 2E9, Canada*

Dipanjan Bhattacharyya − *Department of Biological Sciences, University of Alberta, Edmonton T6G 2E9, Canada*

Alyaa Selim − *Department of Biological Sciences, University of Alberta, Edmonton T6G 2E9, Canada; Department of Pharmacognosy, Faculty of Pharmacy, Sohag University, Sohag 82524, Egypt*

Rupasri Mandal − *Department of Biological Sciences, University of Alberta, Edmonton T6G 2E9, Canada; The Metabolomics Innovation Centre (TMIC), Edmonton T6G 2E9, Canada*

Complete contact information is available at: https://pubs.acs.org/10.1021/acsfoodscitech.4c00298

Author Contributions

This work was conceptualized by DSW and RM. The MagMet-W program was developed and modified by BLL and MR. Experimental work was performed by BLL, MR, YD, ML, MB, HS, AS, and DB. Data analysis was performed by BLL, DB, and AS. Writing-original draft, was performed by BLL, DB, and AS. Writing-reviewing, and editing, was performed by DSW.

Funding

This work was funded by the National Center for Complementary and Integrative Health (NCCIH) and the Office of Dietary Supplements (ODS) of the National Institute of Health (NIH) [U24 AT010811], the Canada Foundation for Innovation (CFI MSIF 42495), and the Alberta Innovates Agri-Food and Bioindustrial Innovation Program (ABIP) (222301549).

Notes

The authors declare no competing financial interest.

■ ACKNOWLEDGMENTS

The authors thank Dr. Marcia LeVatte with her help in editing and preparing this manuscript.

■ ABBREVIATIONS USED

AAS	atomic absorption spectrometry
CE	capillary electrophoresis
CPCA	2-chloropyrimidine-5-carboxylic acid
DSS-d_6	deuterated 2,2-dimethyl-2-silapentane-5 sulfonate
FT-IR	Fourier-transform infrared spectroscopy
GC-MS	gas chromatography mass spectrometry
HPLC	high performance liquid-chromatography
ICP-MS	inductively coupled plasma mass spectrometry
LC-MS	liquid-chromatography mass spectrometry
MagMet-W	Magnetic Resonance for Metabolomics of Wine
MAPE	mean absolute percentage error
NMR	nuclear magnetic resonance
RMSE	root-mean-square error

■ REFERENCES

(1) McGovern, P.; Jalabadze, M.; Batiuk, S.; Callahan, M. P.; Smith, K. E.; Hall, G. R.; Kvavadze, E.; Maghradze, D.; Rusishvili, N.; Bouby, L.; Failla, O.; Cola, G.; Mariani, L.; Boaretto, E.; Bacilieri, R.; This, P.; Wales, N.; Lordkipanidze, D. Early Neolithic wine of Georgia in the South Caucasus. *Proc. Natl. Acad. Sci. U.S.A.* **2017**, *114* (48), E10309−E10318.

(2) Soleas, G. J.; Diamandis, E. P.; Goldberg, D. M. Wine as a biological fluid: History, production, and role in disease prevention. *J. Clin. Lab. Anal.* **1997**, *11* (5), 287−313.

(3) Giacosa, A.; Barale, R.; Bavaresco, L.; Faliva, M. A.; Gerbi, V.; La Vecchia, C.; Negri, E.; Opizzi, A.; Perna, S.; Pezzotti, M.; Rondanelli, M. Mediterranean way of drinking and longevity. *Crit. Rev. Food Sci. Nutr.* **2016**, *56* (4), 635−640.

(4) Golan, R.; Gepner, Y.; Shai, I. Wine and health-new evidence. *Eur. J. Clin. Nutr.* **2019**, *72* (S1), 55−59.

(5) Ferrer-Gallego, R.; Silva, P. The wine industry by-products: applications for food industry and health benefits. *Antioxidants* **2022**, *11* (10), 2025.

(6) Niego, A. G. T.; Lambert, C.; Mortimer, P.; Thongklang, N.; Rapior, S.; Grosse, M.; Schrey, H.; Charria-Girón, E.; Walker, A.; Hyde, K. D.; Stadler, M. The contribution of fungi to the global economy. *Fungal Divers.* **2023**, *121* (1), 95−137.

(7) Zhang, L.; Liu, Q.; Li, Y.; Liu, S.; Tu, Q.; Yuan, C. Characterization of wine volatile compounds from different regions and varieties by HS-SPME/GC-MS coupled with chemometrics. *Curr. Res. Food Sci.* **2023**, *6*, 100418.

(8) Sudraud, P.; Koziet, J. Recherche de nouveaux critères analytiques de caractérisation des vins. *Ann. Nutr. Aliment.* **1978**, *32* (5), 1063−1071.

(9) Swiegers, J. H.; Bartowsky, E. J.; Henschke, P. A.; Pretorius, I. S. Yeast and bacterial modulation of wine aroma and flavour. *Aust. J. Grape Wine Res.* **2005**, *11* (2), 139−173.

(10) Rochfort, S.; Ezernieks, V.; Bastian, S. E. P.; Downey, M. O. Sensory attributes of wine influenced by variety and berry shading discriminated by NMR metabolomics. *Food Chem.* **2010**, *121* (4), 1296−1304.

(11) Ocaña-Rios, I.; Ruiz-Terán, F.; García-Aguilera, M. E.; Tovar-Osorio, K.; de San Miguel, E. R.; Esturau-Escofet, N. Comparison of two sample preparation methods for ^{1}H-NMR wine profiling: Direct analysis and solid-phase extraction. *Vitis* **2021**, *60*, 69−75.

(12) Styger, G.; Prior, B.; Bauer, F. F. Wine flavor and aroma. *J. Ind. Microbiol. Biotechnol.* **2011**, *38* (9), 1145−1159.

(13) Bartella, L.; Bouza, M.; Rocío-Bautista, P.; Di Donna, L.; García-Reyes, J. F.; Molina-Díaz, A. Direct wine profiling by mass spectrometry (MS): a comparison of different ambient MS approaches. *Microchem. J.* **2022**, *179*, 107479.

(14) Gil-Muñoz, R.; Gómez-Plaza, E.; Martínez, A.; López-Roca, J. M. Evolution of phenolic compounds during wine fermentation and post-fermentation: influence of grape temperature. *J. Food Compost. Anal.* **1999**, *12* (4), 259−272.

(15) Borbalán, Á. M. A.; Zorro, L.; Guillén, D. A.; Barroso, C. G. Study of the polyphenol content of red and white grape varieties by liquid chromatography−mass spectrometry and its relationship to antioxidant power. *J. Chromatogr. A* **2003**, *1012* (1), 31−38.

(16) Artero, A.; Artero, A.; Tarín, J. J.; Cano, A. The impact of moderate wine consumption on health. *Maturitas* **2015**, *80* (1), 3−13.

(17) Holt, H. E.; Francis, I. L.; Field, J.; Herderich, M. J.; Iland, P. G. Relationships between wine phenolic composition and wine sensory properties for Cabernet Sauvignon (*Vitis vinifera* L.). *Aust. J. Grape Wine Res.* **2008**, *14* (3), 162−176.

(18) Serra-Cayuela, A.; Jourdes, M.; Riu-Aumatell, M.; Buxaderas, S.; Teissedre, P.-L.; López-Tamames, E. Kinetics of browning, phenolics, and 5-hydroxymethylfurfural in commercial sparkling wines. *J. Agric. Food Chem.* **2014**, *62* (5), 1159−1166.

(19) Lambert, M.; Meudec, E.; Verbaere, A.; Mazerolles, G.; Wirth, J.; Masson, G.; Cheynier, V.; Sommerer, N. A high-throughput UHPLC-QqQ-MS method for polyphenol profiling in rosé wines. *Molecules* **2015**, *20* (5), 7890−7914.

(20) Suprun, A. R.; Dubrovina, A. S.; Tyunin, A. P.; Kiselev, K. V. Profile of stilbenes and other phenolics in Fanagoria white and red Russian wines. *Metabolites* **2021**, *11* (4), 231.

(21) Catharino, R. R.; Cunha, I. B. S.; Fogaça, A. O.; Facco, E. M. P.; Godoy, H. T.; Daudt, C. E.; Eberlin, M. N.; Sawaya, A. C. H. F. Characterization of must and wine of six varieties of grapes by direct infusion electrospray ionization mass spectrometry. *J. Mass Spectrom.* **2006**, *41* (2), 185−190.

(22) Hartmanova, L.; Ranc, V.; Papouskova, B.; Bednar, P.; Havlicek, V.; Lemr, K. Fast profiling of anthocyanins in wine by desorption nano-electrospray ionization mass spectrometry. *J. Chromatogr. A* **2010**, *1217* (25), 4223−4228.

(23) Rubert, J.; Lacina, O.; Fauhl-Hassek, C.; Hajslova, J. Metabolic fingerprinting based on high-resolution tandem mass spectrometry: a reliable tool for wine authentication? *Anal. Bioanal. Chem.* **2014**, *406* (27), 6791−6803.

(24) Bi, H.; Xi, M.; Zhang, R.; Wang, C.; Qiao, L.; Xie, J. Electrostatic spray ionization-mass spectrometry for direct and fast wine characterization. *ACS Omega* **2018**, *3* (12), 17881−17887.

(25) Valls Fonayet, J.; Loupit, G.; Richard, T. MS- and NMR-metabolomic tools for the discrimination of wines: Applications for authenticity. *Adv. Bot. Res.* **2021**, *98*, 297−357.

(26) Solovyev, P. A.; Fauhl-Hassek, C.; Riedl, J.; Esslinger, S.; Bontempo, L.; Camin, F. NMR spectroscopy in wine authentication: an official control perspective. *Compr. Rev. Food Sci. Food Saf.* **2021**, *20* (2), 2040−2062.

(27) Viskić, M.; Bandić, L. M.; Korenika, A. M. J.; Jeromel, A. NMR in the service of wine differentiation. *Foods* **2021**, *10* (1), 120.

(28) Le Mao, I.; Da Costa, G.; Bautista, C.; de Revel, G.; Richard, T. Application of ^{1}H NMR metabolomics to French sparkling wines. *Food Control* **2023**, *145*, 109423.

(29) Le Mao, I.; Da Costa, G.; Richard, T. ^{1}H-NMR metabolomics for wine screening and analysis. *OENO One* **2023**, *57* (1), 15−31.

(30) Gougeon, L.; Da Costa, G.; Le Mao, I.; Ma, W.; Teissedre, P.-L.; Guyon, F.; Richard, T. Wine analysis and authenticity using ^{1}H-NMR metabolomics data: Application to Chinese wines. *Food Anal. Methods* **2018**, *11* (12), 3425−3434.

(31) Prakash, S.; Iturmendi, N.; Grelard, A.; Moine, V.; Dufourc, E. Quantitative analysis of Bordeaux red wine precipitates by solid-state NMR: role of tartrates and polyphenols. *Food Chem.* **2016**, *199*, 229−237.

(32) Matviychuk, Y.; Haycock, S.; Rutan, T.; Holland, D. J. Quantitative analysis of wine and other fermented beverages with benchtop NMR. *Anal. Chim. Acta* **2021**, *1182*, 338944.

(33) Dumez, J. N. NMR methods for the analysis of mixtures. *Chem. Commun.* **2022**, *58* (100), 13855−13872.

https://doi.org/10.1021/acsfoodscitech.4c00298
ACS Food Sci. Technol. 2024, 4, 1937−1949

(34) Lindon, J. C.; Nicholson, J. K.; Everett, J. R. NMR spectroscopy of biofluids. *Annu. Rep. NMR Spectrosc.* **1999**, *38* (C), 1−88.
(35) Spraul, M.; Link, M.; Schaefer, H.; Fang, F.; Schuetz, B. Wine analysis to check quality and authenticity by fully-automated ^{1}H-NMR. *BIO Web Conf.* **2015**, *5* (23), 02022.
(36) Bruker. Wine-Profiling™ 4.0. https://www.bruker.com/en/products-and-solutions/mr/nmr-food-solutions/wine-profiling0/_jcr_content/root/sections/more_information/sectionpar/linklist/contentpar-1/calltoaction.download-asset.PDF/links/item0/FoodScreener%20Wine%20Profiling%20Brochure.PDF, (accessed Jan 14, 2024).
(37) Lee, B. L.; Rout, M.; Mandal, R.; Wishart, D. S. Automated identification and quantification of metabolites in human fecal extracts by nuclear magnetic resonance spectroscopy. *Magn. Reson. Chem.* **2023**, *61* (12), 705−717.
(38) Rout, M.; Lipfert, M.; Lee, B. L.; Berjanskii, M.; Assempour, N.; Fresno, R. V.; Cayuela, A. S.; Dong, Y.; Johnson, M.; Shahin, H.; Gautam, V.; Sajed, T.; Oler, E.; Peters, H.; Mandal, R.; Wishart, D. S. MagMet: a fully automated web server for targeted nuclear magnetic resonance metabolomics of plasma and serum. *Magn. Reson. Chem.* **2023**, *61* (12), 681−704.
(39) Weljie, A. M.; Newton, J.; Mercier, P.; Carlson, E.; Slupsky, C. M. Targeted profiling: quantitative analysis of ^{1}H NMR metabolomics data. *Anal. Chem.* **2006**, *78* (13), 4430−4442.
(40) Helmus, J. J.; Jaroniec, C. P. Nmrglue: an open source Python package for the analysis of multidimensional NMR data. *J. Biomol. NMR* **2013**, *55* (4), 355−367.
(41) Schober, D.; Jacob, D.; Wilson, M.; Cruz, J. A.; Marcu, A.; Grant, J. R.; Moing, A.; Deborde, C.; De Figueiredo, L. F.; Haug, K.; Rocca-Serra, P.; Easton, J.; Ebbels, T. M. D.; Hao, J.; Ludwig, C.; Günther, U. L.; Rosato, A.; Klein, M. S.; Lewis, I. A.; Luchinat, C.; Jones, A. R.; Grauslys, A.; Larralde, M.; Yokochi, M.; Kobayashi, N.; Porzel, A.; Griffin, J. L.; Viant, M. R.; Wishart, D. S.; Steinbeck, C.; Salek, R. M.; Neumann, S. NmrML: a community supported open data standard for the description, storage, and exchange of NMR data. *Anal. Chem.* **2018**, *90* (1), 649−656.
(42) Papotti, G.; Bertelli, D.; Graziosi, R.; Silvestri, M.; Bertacchini, L.; Durante, C.; Plessi, M. Application of one- and two-dimensional NMR spectroscopy for the characterization of protected designation of Origin Lambrusco wines of Modena. *J. Agric. Food Chem.* **2013**, *61* (8), 1741−1746.
(43) Pereira, G. E.; Gaudillère, J.-P.; Van Leeuwen, C.; Hilbert, G.; Maucourt, M.; Deborde, C.; Moing, A.; Rolin, D. ^{1}H-NMR metabolic profiling of wines from three cultivans, three soil types and two contrasting vintages. *OENO One* **2007**, *41* (2), 103−109.
(44) Zhu, J.; Hu, B.; Lu, J.; Xu, S. Analysis of metabolites in Cabernet Sauvignon and Shiraz dry red wines from Shanxi by ^{1}H NMR spectroscopy combined with pattern recognition analysis. *Open Chem.* **2018**, *16* (1), 446−452.
(45) Aru, V.; Sørensen, K. M.; Khakimov, B.; Toldam-Andersen, T. B.; Balling Engelsen, S. Cool-climate red wines-chemical composition and comparison of two protocols for ^{1}H-NMR analysis. *Molecules* **2018**, *23* (1), 160.
(46) Tredwell, G. D.; Bundy, J. G.; De Iorio, M.; Ebbels, T. M. D. Modelling the acid/base ^{1}H NMR chemical shift limits of metabolites in human urine. *Metabolomics* **2016**, *12* (10), 152.
(47) Voehler, M. W.; Collier, G.; Young, J. K.; Stone, M. P.; Germann, M. W. Performance of cryogenic probes as a function of ionic strength and sample tube geometry. *J. Magn. Reson.* **2006**, *183* (1), 102−109.
(48) Mckay, R. T. How the 1D-NOESY suppresses solvent signal in metabonomics NMR spectroscopy: an examination of the pulse sequence components and evolution. *Concepts Magn. Reson., Part A: Bridging Educ. Res.* **2011**, *38* (5), 197−220.
(49) Le Mao, I.; Martin-Pernier, J.; Bautista, C.; Lacampagne, S.; Richard, T.; Da Costa, G. ^{1}H-NMR metabolomics as a tool for winemaking monitoring. *Molecules* **2021**, *26* (22), 6771.
(50) Lee, J. E.; Hwang, G. S.; Van Den Berg, F.; Lee, C. H.; Hong, Y. S. Evidence of vintage effects on grape wines using ^{1}H NMR-based metabolomic study. *Anal. Chim. Acta* **2009**, *648* (1), 71−76.
(51) Mascellani, A.; Hoca, G.; Babisz, M.; Krska, P.; Kloucek, P.; Havlik, J. ^{1}H NMR chemometric models for classification of Czech wine type and variety. *Food Chem.* **2021**, *339*, 127852.
(52) Son, H.-S.; Hwang, G.-S.; Kim, K. M.; Kim, E.-Y.; van den Berg, F.; Park, W.-M.; Lee, C.-H.; Hong, Y.-S. ^{1}H NMR-based metabolomic approach for understanding the fermentation behaviors of wine yeast strains. *Anal. Chem.* **2009**, *81* (3), 1137−1145.
(53) Bambina, P.; Spinella, A.; Lo Papa, G.; Chillura Martino, D. F.; Lo Meo, P.; Corona, O.; Cinquanta, L.; Conte, P. ^{1H} NMR-based metabolomics to assess the impact of soil type on the chemical composition of Nero d'Avola red wines. *J. Agric. Food Chem.* **2023**, *71* (14), 5823−5835.
(54) Cassino, C.; Tsolakis, C.; Bonello, F.; Gianotti, V.; Osella, D. Effects of area, year and climatic factors on Barbera wine characteristics studied by the combination of ^{1}H-NMR metabolomics and chemometrics. *J. Wine Res.* **2017**, *28* (4), 259−277.
(55) Nilsson, M.; Duarte, I. F.; Almeida, C.; Delgadillo, I.; Goodfellow, B. J.; Gil, A. M.; Morris, G. A. High-resolution NMR and diffusion-ordered spectroscopy of port wine. *J. Agric. Food Chem.* **2004**, *52* (12), 3736−3743.
(56) López-Rituerto, E.; Savorani, F.; Avenoza, A.; Busto, J. H.; Peregrina, J. M.; Engelsen, S. B. Investigations of la Rioja terroir for wine production using ^{1}H NMR metabolomics. *J. Agric. Food Chem.* **2012**, *60* (13), 3452−3461.
(57) Son, H.-S.; Kim, K. M.; van den Berg, F.; Hwang, G.-S.; Park, W.-M.; Lee, C.-H.; Hong, Y.-S. ^{1}H nuclear magnetic resonance-based metabolomic characterization of wines by grape varieties and production areas. *J. Agric. Food Chem.* **2008**, *56* (17), 8007−8016.
(58) Son, H. S.; Hwang, G. S.; Kim, K. M.; Ahn, H. J.; Park, W. M.; Van Den Berg, F.; Hong, Y. S.; Lee, C. H. Metabolomic studies on geographical grapes and their wines using ^{1}H NMR analysis coupled with multivariate statistics. *J. Agric. Food Chem.* **2009**, *57* (4), 1481−1490.
(59) Anastasiadi, M.; Zira, A.; Magiatis, P.; Haroutounian, S. A.; Skaltsounis, A. L.; Mikros, E. ^{1}H NMR-based metabonomics for the classification of Greek wines according to variety, region, and vintage. Comparison with HPLC data. *J. Agric. Food Chem.* **2009**, *57* (23), 11067−11074.
(60) Ali, K.; Maltese, F.; Toepfer, R.; Choi, Y. H.; Verpoorte, R. Metabolic characterization of Palatinate German white wines according to sensory attributes, varieties, and vintages using NMR spectroscopy and multivariate data analyses. *J. Biomol. NMR* **2011**, *49* (3−4), 255−266.
(61) Hu, B.; Gao, J.; Xu, S.; Zhu, J.; Fan, X.; Zhou, X. Quality evaluation of different varieties of dry red wine based on nuclear magnetic resonance metabolomics. *Appl. Biol. Chem.* **2020**, *63* (1), 24.
(62) Waterhouse, A. L.; Sacks, G. L.; Jeffery, D. W. *Understanding Wine Chemistry*; Wiley, 2016.
(63) Nikolantonaki, M.; Magiatis, P.; Waterhouse, A. L. Direct analysis of free and sulfite-bound carbonyl compounds in wine by two-dimensional quantitative proton and carbon nuclear magnetic resonance spectroscopy. *Anal. Chem.* **2015**, *87* (21), 10799−10806.
(64) Cassino, C.; Tsolakis, C.; Gulino, F.; Vaudano, E.; Osella, D. The effects of sulphur dioxide on wine metabolites: New insights from ^{1}H NMR spectroscopy based *in-situ* screening, detection, identification and quantification. *LWT—Food Sci. Technol.* **2021**, *145*, 111296.
(65) Romano, P.; Brandolini, V.; Ansaloni, C.; Menziani, E. The production of 2,3-butanediol as a differentiating character in wine yeasts. *World J. Microbiol. Biotechnol.* **1998**, *14* (5), 649−653.
(66) Evers, M. S.; Roullier-Gall, C.; Morge, C.; Sparrow, C.; Gobert, A.; Alexandre, H. Vitamins in wine: Which, what for, and how much? *Compr. Rev. Food Sci. Food Saf.* **2021**, *20* (3), 2991−3035.
(67) Cibrario, A.; Perello, M. C.; Miot-Sertier, C.; Riquier, L.; de Revel, G.; Ballestra, P.; Dols-Lafargue, M. Carbohydrate composition

of red wines during early aging and incidence on spoilage by *Brettanomyces bruxellensis*. *Food Microbiol.* **2020**, *92*, 103577.
(68) Agustini, B. C.; de Lima, D. B.; Bonfim, T. M. B. Composition of amino acids and bioactive amines in common wines of Brazil. *Acta Sci., Health Sci.* **2014**, *36* (2), 225−233.
(69) Gutiérrez-Escobar, R.; Aliaño-González, M. J.; Cantos-Villar, E. Wine polyphenol content and its influence on wine quality and properties: A review. *Molecules* **2021**, *26* (3), 718.
(70) Alcohol Drinking *IARC Monographs on the Evaluation of the Carcinogenic Risks to Humans*; lnternational Agency for Research on Cancer, 1988; Vol. *44*.
(71) Patterson, K. Y.; Bhagwat, S.; Williams, J. R.; Howe, J. C.; Holden, J. M.; Zeisel, S. H.; Dacosta, K. A.; Mar, M.-H. *USDA Database for the Choline Content of Common Foods, Release 2*, 2008.
(72) Román, T.; Nicolini, G.; Barp, L.; Malacarne, M.; Tait, F.; Larcher, R. Shikimic acid concentration in white wines produced with different processing protocols from fungus-resistant grapes growing in the Alps. *Vitis* **2018**, *57* (2), 41−46.
(73) Pfeiffer, P.; König, H. Pyroglutamic acid: A novel compound in wines. In *Biology of Microorganisms on Grapes, in Must and in Wine*; Springer, 2009; pp 233−240.
(74) Soufleros, E. H.; Bouloumpasi, E.; Zotou, A.; Loukou, Z. Determination of biogenic amines in Greek wines by HPLC and ultraviolet detection after dansylation and examination of factors affecting their presence and concentration. *Food Chem.* **2007**, *101* (2), 704−716.
(75) Pfeiffer, P.; Radler, F. Determination of ethanolamine in wine by HPLC after derivatization with 9-fluorenylmethoxycarbonylchloride. *Am. J. Enol. Vitic.* **1992**, *43* (4), 315−317.
(76) Gerginova, D.; Simova, S. Chemical profiling of wines produced in Bulgaria and distinction from international grape varieties. *ACS Omega* **2023**, *8* (21), 18702−18713.
(77) Mar, M.-H.; Zeisel, S. H. Betaine in wine: answer to the French paradox? *Med. Hypotheses* **1999**, *53* (5), 383−385.
(78) Herbert, P.; Santos, L.; Alves, A. Simultaneous quantification of primary, secondary amino acids, and biogenic amines in musts and wines using OPA/3-MPA/FMOC-CI fluorescent derivatives. *J. Food Sci.* **2001**, *66* (9), 1319−1325.
(79) Onache, P. A.; Florea, A.; Geana, E.-I.; Ciucure, C. T.; Ionete, R. E.; Sumedrea, D. I.; Tiţa, O. Assessment of bioactive phenolic compounds in musts and the corresponding wines of white and red grape varieties. *Appl. Sci.* **2023**, *13* (9), 5722.
(80) Bourgeois, J. F.; McColl, I.; Barja, F. Formic acid, acetic acid and methanol: their relevance to the verification of the authenticity of vinegar. *Arch. Sci.* **2006**, *59* (1), 107−112.
(81) Medeiros, J.; Xu, S.; Pickering, G. J.; Kemp, B. S. Influence of caffeic and caftaric acid, fructose, and storage temperature on furan derivatives in base wine. *Molecules* **2022**, *27* (22), 7891.
(82) Konakovsky, V.; Focke, M.; Hoffmann-Sommergruber, K.; Schmid, R.; Scheiner, O.; Moser, P.; Jarisch, R.; Hemmer, W. Levels of histamine and other biogenic amines in high-quality red wines. *Food Addit. Contam.: Part A* **2011**, *28* (4), 408−416.
(83) International Organisation of Vine and Wine. *International Code of Oenological Practices*, 2024.
(84) International Organisation of Vine and Wine. *Resolution OIV-OENO 581A-2021: Treatment with Fumaric Acid in Wine to Inhibit Malolactic Fermentation*, 2021.
(85) Lengyel, E.; Sikolya, L. Authenticity tests of white wines from the Apold Depression. *Manage. Sustainable Dev.* **2014**, *6* (2), 55−59.

https://doi.org/10.1021/acsfoodscitech.4c00298
ACS Food Sci. Technol. 2024, 4, 1937−1949